Journal of Food Engineering 162 (2015) 9–17

Contents lists available at ScienceDirect

Journal of Food Engineering

journal homepage: www.elsevier.com/locate/jfoodeng

A method to construct fruit maturity color scales based on support machines for regression: Application to olives and grape seeds

Felipe Avila [a,*,1], Marco Mora [a,*,1], Miguel Oyarce [a,1], Alex Zuñiga [a,1], Claudio Fredes [b,1]

[a] Department of Computer Science, Universidad Católica del Maule, Talca, Chile
[b] Department of Agricultural Science, Universidad Católica del Maule, Curicó, Chile

ARTICLE INFO

Article history:
Received 24 March 2014
Received in revised form 23 November 2014
Accepted 31 March 2015
Available online 11 April 2015

Keywords:
Color scales
Fruit maturity
Support Vector Regression

ABSTRACT

Color scales are a powerful tool used in agriculture for estimate maturity of fruits. Fruit maturity is an important parameter to determine the harvest time. Typically, to obtain the maturity grade, a human expert visually associates the fruit color with a color present in the scale. In this paper, a computer-based method to create color scales is proposed. The proposed method performs a multidimensional regression based on Support Vector Regression (SVR) to generate color scales. The experimentation considers two color scales examples, the first one for grape seeds, the second one for olives. Grape seed data set contains 250 samples and olives data set has 200 samples. Color scales developed by SVR were validated through K-fold Cross Validation method, using mean squared error as performance function. The proposed method generates scales that adequately follow the evolution of color in the fruit maturity process, provides a tool to define different phenolic pre-harvest stages, which may be of interest to the human expert.

1. Introduction

Color is one of the most important characteristics of food products. Consumers are influenced by this parameter; they tend to prefer products that have vivid colors and uniforms (Lee et al., 2013). Because of this, the food industry had developed methods to objectively measure color using this parameter to estimate the quality of the products (Wu and Sun, 2013).

The color is closely related to chemical and physical properties of food (Sant'Anna et al., 2013). Particularly, the phenolic state of a food is important because this is associated with the product quality (Zhenfeng et al., 2009). In fruits, the phenolic state estimation has been widely studied (Garitta et al., 2008), since certain stages of maturity can be related to the concentration of antioxidants and other beneficial substances to health (Palafox-Carlos et al., 2012; Mazur et al., 2013).

Determining the right point of maturity in fruits is traditionally performed by a human expert. This process is very prone to error due to factors such as fatigue, distraction or boredom by the expert (Changyong et al., 2009). In the field of estimation of maturity, has become increasingly important digital image analysis, due to its simplicity and low cost (Brosnan and Sun, 2002). Determining the state of maturity by computer vision has been studied on a variety of fruits. In Intaravanne et al. (2012) a spectral analysis of images of bananas obtained under white light and ultra-violet is performed. The images obtained are used to classify areas of the banana that are immature, mature and over-mature. Similar work is shown in Slaughter et al. (2013), where the color of the bulb is used as a predictive indicator of the maturity and quality of flavor. This analysis is carried out by a spectroscope, an instrument which enables the analysis in the visible spectrum and the near infrared. In another study with bananas (Mendoza and Aguilera, 2004), the stage of fruit maturity is estimated by analyzing the color, stains and, texture in the image. In Pace et al. (2013) a Computer Vision System to estimate the antioxidant and phenol content on carrots based on the fruit's surface color was performed. The color is determined by the center of mass of the two-dimensional histogram considering channels “a” and “b” (CIE Lab color space.) In Pedreschi et al. (2006) a low cost Computer Vision System to measure a foodstuff's color of heterogeneous form and color was designed and implemented. In Choi et al. (1995) an index of the tomato's ripeness is proposed, which allows classifying the fresh fruit into 6 classes, according to the USDA international standard. The tomato images are transformed to the HSI color model, and the information of the H channel tone is used to build the proposed

* Corresponding authors.
E-mail addresses: favila@litrp.cl (F. Avila), mora@spock.ucm.cl, marcomoracofre@gmail.com (M. Mora), moyarce@litrp.cl (M. Oyarce), azuniga@litrp.cl (A. Zuñiga), cfredes@ucm.cl (C. Fredes).
URL: http://www.ganimides.ucm.cl/mmora (M. Mora).
[1] Address: Laboratory of Technological Research on Pattern Recognition, Universidad Católica del Maule, Avenida San Miguel 3605, Talca, Chile, www.litrp.cl.

http://dx.doi.org/10.1016/j.jfoodeng.2015.03.035
0260-8774/

index. Previous studies show that the color obtained from digital images is a strong indicator to estimate the fruit ripeness and quality. In Vanloot et al. (2014) a Computer Vision System to discriminate varieties of French olives is developed (Aglandau, Bouteillan, Lucques, Picholine and Tanche). Pit images (frontal and profile) were used, characteristics such as the histograms of the RGB model and form descriptors (area, perimeter, length, width, etc.) were computed. The classification is performed by Partial Least Squares Discriminant Analysis. In Guzmán et al. (2013) table olives considering 2 types of images are analyzed. The segmentation is performed on infrared images, and the olives are classified into 5 categories according to the percentage of faulty pixels on the optical image. In Diaz et al. (2000) a CVS to classify table olives (Manzanilla variety) into 4 categories is presented. Characteristics of the CIE Lab model are used, and the classification is performed by means of a fast algorithm based on Mahalanobis distance. As reflected in previous studies, the color of the fruits is a robust indicator of the maturity. Furthermore it is deduced that developing color scales is a fundamental task if it is desired to relate the color and ripeness of the fruit.

As was previously seen a large number of works to estimate the maturity based on digital image analysis have been proposed. While these works are of great support for decision-making, most cannot determine intermediate stages of fruit maturity. Due this, the development of color scales is of great interest, since these provide a method for the human expert to define intermediate stages of fruit maturity. In the literature several works have been proposed to develop color scales and monitor maturity of fruits. In Dah-Jye et al. (2008) a scale with 12 levels of maturity for Medjool are proposed. Each level of maturity corresponds to a range of colors in the *RGB* space. The scale corresponds to a continuous curve in the color space, which is constructed based on a linearization of the *RGB* model. While this method has acceptable results, is strongly influenced by the selection conditions of the fruit. Furthermore, for a proper generalization is necessary to obtain a large number of samples. Similar work is presented in Wang et al. (2012), where a color scale is developed to determine the optimum harvesting of cherries. In Ristic and Iland (2005) a study of the color of the grape seed is made, and a color scale for strain "Shiraz" is constructed. The previous work shows a high correlation between color, texture and shape of the seed relative to the ripeness of the grapes. Taking as reference the previous work, Fredes et al. (2010) it is proposes compare the color of the seed with a color scale, which was developed in the same work.

The construction of the scale manually is prone to errors by the author of the scale. For this reason, it is interesting to develop a method to generate color scales automatically based on samples obtained on different dates to later determine the maturity.

This paper proposes a method to develop color scales automatically based on Support Vector Machines (SVM) for regression, which have good results in very complex data sets. Examples on grape seeds and olives are presented in the work. The scales developed by the method allow associating the color of the fruit with ripeness. The rest of the paper is organized as follows: Section 2 provides an overview of the proposed method and presents experiments. The results are presented in Section 3. Finally Section 4 concludes this work.

2. Material and methods

The proposed method to construct color scales consider four main stages (Fig. 1):

- Stage 1: Image Acquisition.
- Stage 2: Automatic Segmentation robust to shadow and highlights.
- Stage 3: Representative color estimation.
- Stage 4: Color scale construction using SVR model.

In this paper two color scales of maturity of fruits were developed, using for the experimentation Matlab R2010a (MathWorks Inc. ©, Natick, MA, US) and the Image Processing Toolbox. A maturity scale for olive and another scale for the maturity of the grape seed. The images of each of the fruits were acquired during the entire period of phenolic maturity in which noticeable changes in color occurs. Due to the physical differences of grape seed and olive, samples are acquired using two different instruments. In the case of grape seeds, the images were acquired using a conventional scanner (Canon Mg-3110) in order to take a large number of samples, as shown in Fig. 2(a). For the case of olives, the images

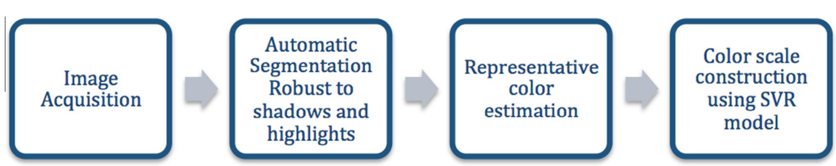

Fig. 1. Block diagram of the method: In this figure four stages of the method are presented.

(a) Scanner (b) Camera

Fig. 2. Acquisition of samples.

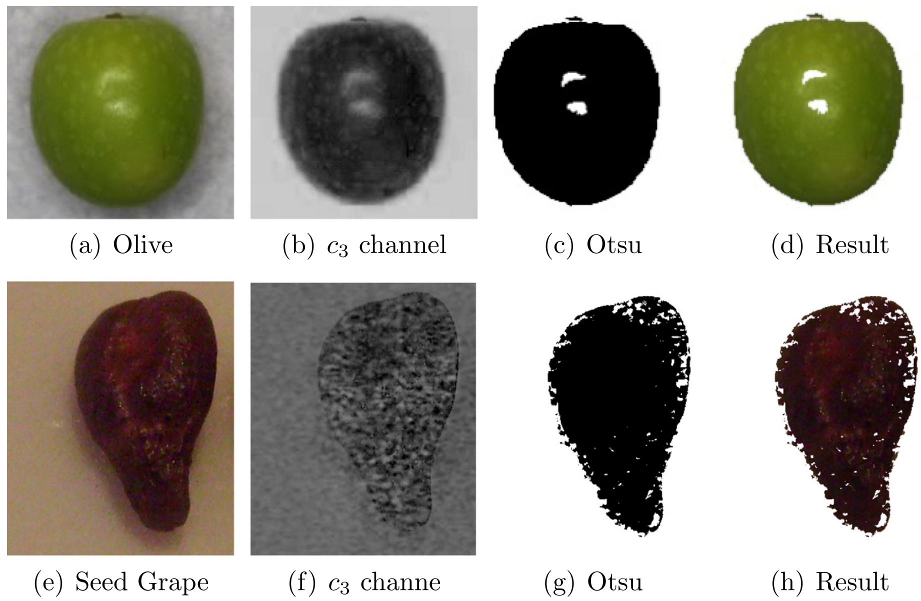

Fig. 3. Segementation process.

were acquired using a digital camera (Canon Eos Rebel T3, Lens Ef-s 18-55), which is maintained at a constant height of the fruit (20 cm) using a tripod, as shown in Fig. 2(b). Through this method for capture two dataset was obtained. In the case of grape seed data set of 250 samples was obtained, while for olives a dataset of 200 samples was obtained.

2.1. Segmentation and obtaining representative color

After the acquisition, a preprocessing stage of the images was implemented due to two problems: the shadows and highlights. The images are transformed from *RGB* color model to a invariant illumination color model $c_1c_2c_3$ (Gevers, 1999). This color model has been used in the literature to implement steps of the image segmentation with the aforementioned defects (Salvador et al., 2001). The expression of the $c_1c_2c_3$ model is the next:

$$c1_{i,j} = \arctan\frac{R_{i,j}}{\text{máx}(G_{i,j}, B_{i,j})} \tag{1}$$

$$c2_{i,j} = \arctan\frac{G_{i,j}}{\text{máx}(R_{i,j}, B_{i,j})} \tag{2}$$

$$c3_{i,j} = \arctan\frac{B_{i,j}}{\text{máx}(G_{i,j}, R_{i,j})} \tag{3}$$

where $R_{i,j}$, $G_{i,j}$, and $B_{i,j}$ represent the components red, green, and blue of a pixel (i,j). With the image in the invariant color model is possible obtain a robust segmentation for the problems mentioned above.

The segmentation stage was performed using the well known method of Otsu (1979). This method is an iterative algorithm that performs a non-parametric thresholding, where the optimal threshold of segmentation is obtained by maximizing the variance between different gray levels present in the image. Fig. 3 shows the complete process of segmentation. Fig. 3(a) and (e) shows the original images of olive and seed respectively, which contain shadows and light bumps. Channel c_3 for segmentation is chosen, given the good results obtained in previous work (Avila et al., 2014). Fig. 3(b) and (f) shows images of the c_3 channel of invariant color model $c_1c_2c_3$. Fig. 3(c) and (g) shows the automatic thresholding of the channel c_3 using Otsu method. Finally, Fig. 3(d) and (h) shows the pixels segmented in both

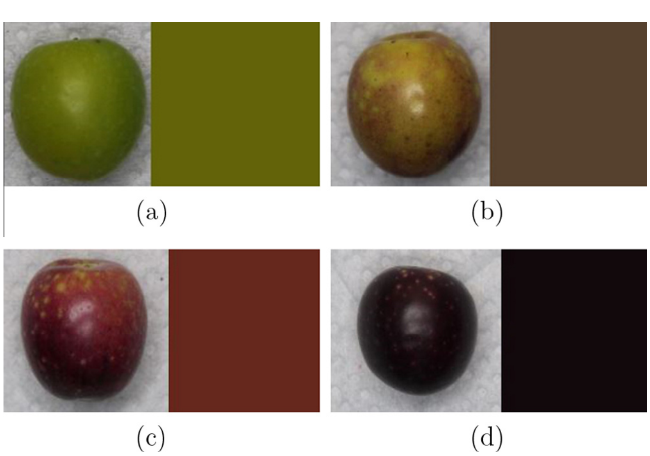

Fig. 4. Estimated representative colors. (For interpretation of the references to colour in this figure legend, the reader is referred to the web version of this article.)

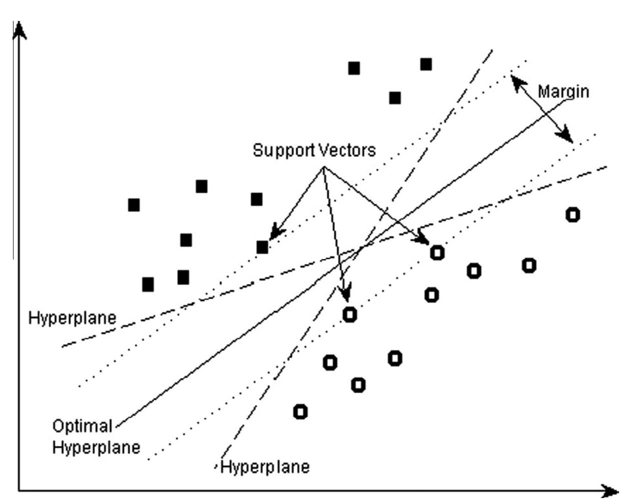

Fig. 5. Support vectors for classification.

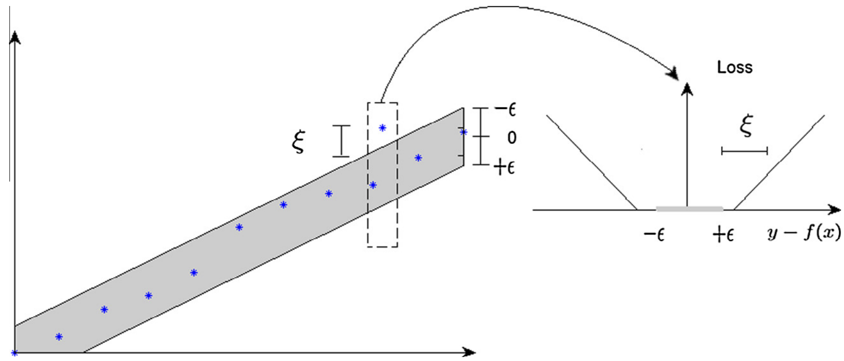

Fig. 6. Support vector regression.

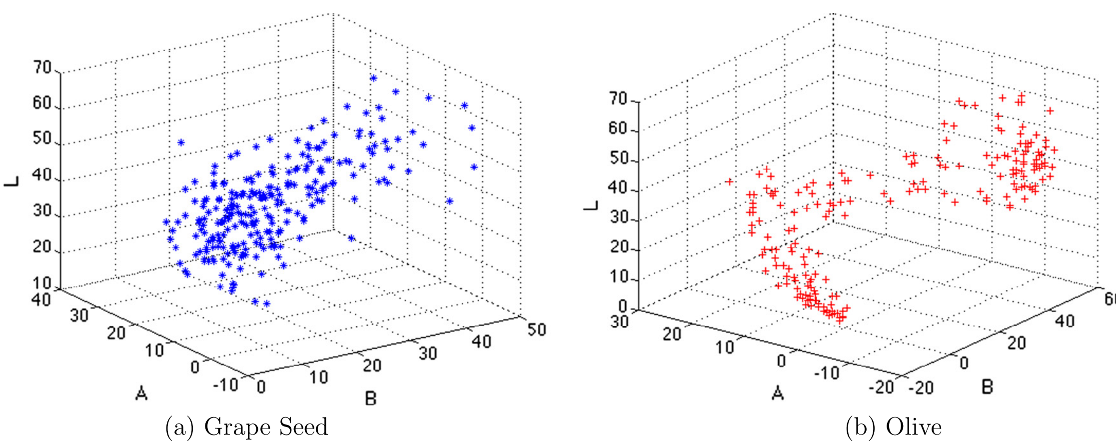

Fig. 7. Data set how points in $\mathbf{R}^3$.

Table 1
Performance obtained by using K-fold cross validation on the data of olives. The rows show the MSE for each model using the respective fold. Bold notation indicate which fold was selected to be used as the model that generated the color scale.

Fold	Model 1	Model 2
1	8.22	31.01
2	19.91	37.82
3	14.74	32.52
4	**5.52**	20.82
5	18.16	38.07
6	9.36	24.74
7	6.47	**12.40**
8	6.63	20.04
9	13.78	32.14
10	10.32	25.60

Table 2
Performance obtained by using K-fold cross validation on the data from grape seeds. The rows show the MSE for each model using the respective fold. Bold notation indicate which fold was selected to be used as the model that generated the color scale.

Fold	Model 1	Model 2
1	**33.92**	33.41
2	40.18	26.69
3	51.83	28.85
4	38.05	34.72
5	49.21	39.99
6	56.81	**22.64**
7	43.48	37.58
8	39.54	28.60
9	68.07	25.76
10	79.33	35.41

fruits. From these last two images one can observe that thse problems shock of light and shadow were properly dealt with by the proposed segmentation stage.

After the segmentation step, the representative color for all images data sets is estimated. To obtain a representative color, the median is calculated. The median is chosen since it is a robust estimator for the outliers to determine the central tendency of a population. The computation of the median requires an ordering of the data, which on color images results in a system of vectors (this is due to the colors are not scalar values but vectors in $\mathbf{R}^3$), which is a quite complex problem. It is chosen for the ordering of the colors, an algorithm proven to be effective for this purpose (Hanbury and Serra, 2011). With the sorted vectors, the median of these vectors is chosen as representative color of the fruit. Fig. 4 shows the estimated representative color for four olives in different stages of maturation. It can be seen that the result of the method of vector matches the visual appreciation of the representative color.

2.2. Color scale based on support machines for regression

The Support Vector Machines (SVM) is a machine learning technique based on kernels originally proposed by Cortes and Vapnik (1995). In its simplest form the SVM are linear classifiers, in which data are separated by a hyperplane which is defined by a number of support vectors. These support vectors are part of the training set and are used to define the boundaries of the two classes. In Fig. 5 we can appreciate both, the support vectors and the hyperplane separating the two types, which are defined by the circles and boxes.

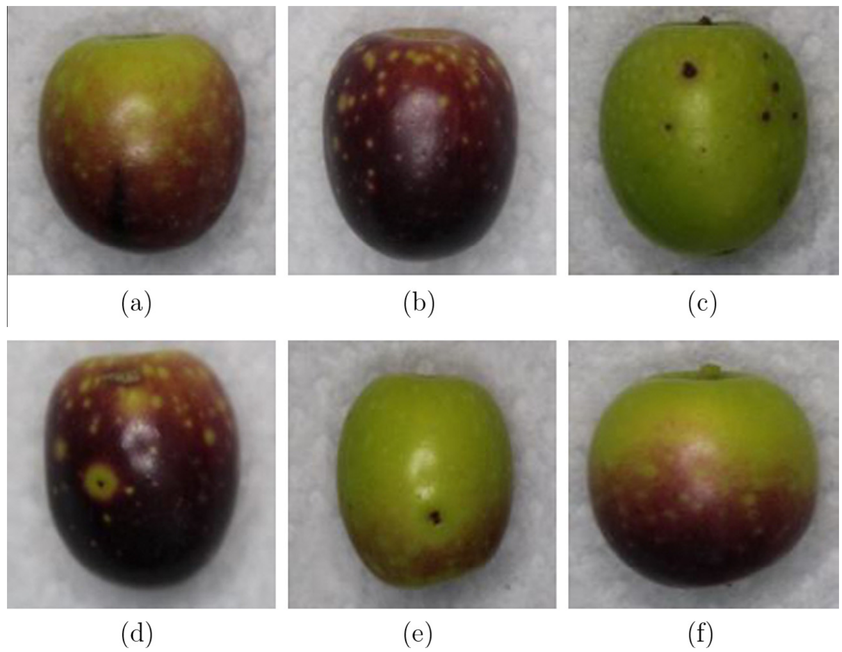

Fig. 8. Examples of olives in different maturity stages.

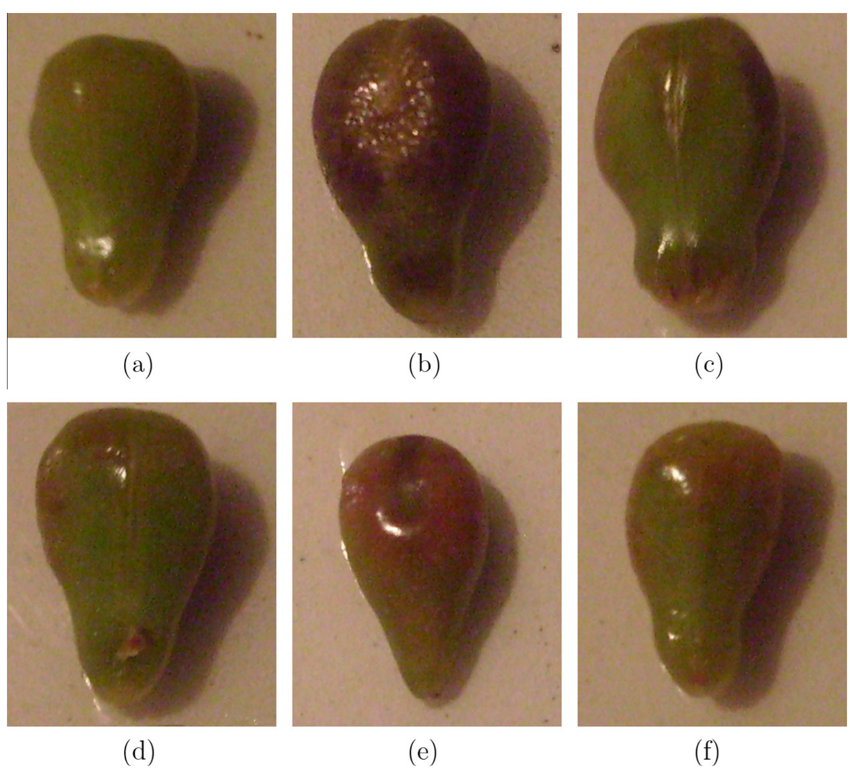

Fig. 9. Examples of grape seeds in different maturity stages.

Traditionally, the SVM allow only dealing with outputs of binary type. However, when looking to work with continuous response values, is necessary to generalize the algorithm of support machine. Similarly to the case of classification, a margin is constructed in the space of the target values y. This range becomes a tube, as seen in Fig. 6 of radius ϵ fitted to the data.

The adjustment between the model complexity and the points outside the tube is given by the following minimization problem:

$$\begin{aligned}
&\underset{\mathbf{w}\in H,\xi^{(*)}\in\mathbf{R}^m,b\in\mathbf{R}}{\text{minimize}}\ \tau(\mathbf{w},\xi^*) = \frac{1}{2}\|\mathbf{w}\|^2 + C\sum_{i=1}^{m}\xi_i + \xi_i^* \\
&\text{subject to } f(\mathbf{x}_i) - y_i \leqslant \epsilon + \xi_i \\
&\qquad\qquad y_i - f(\mathbf{x}_i) \leqslant \epsilon + \xi_i \\
&\qquad\qquad \xi_i, \xi_i^* \geqslant 0 \qquad\qquad \text{for all } i = 1,\ldots,m.
\end{aligned}$$

where C is a predefined value, ξ and ξ^* correspond to two slack variables for the two cases $f(\mathbf{x}_i) - y_i > \epsilon$ and $y_i - f(\mathbf{x}_i) > \epsilon$ respectively.

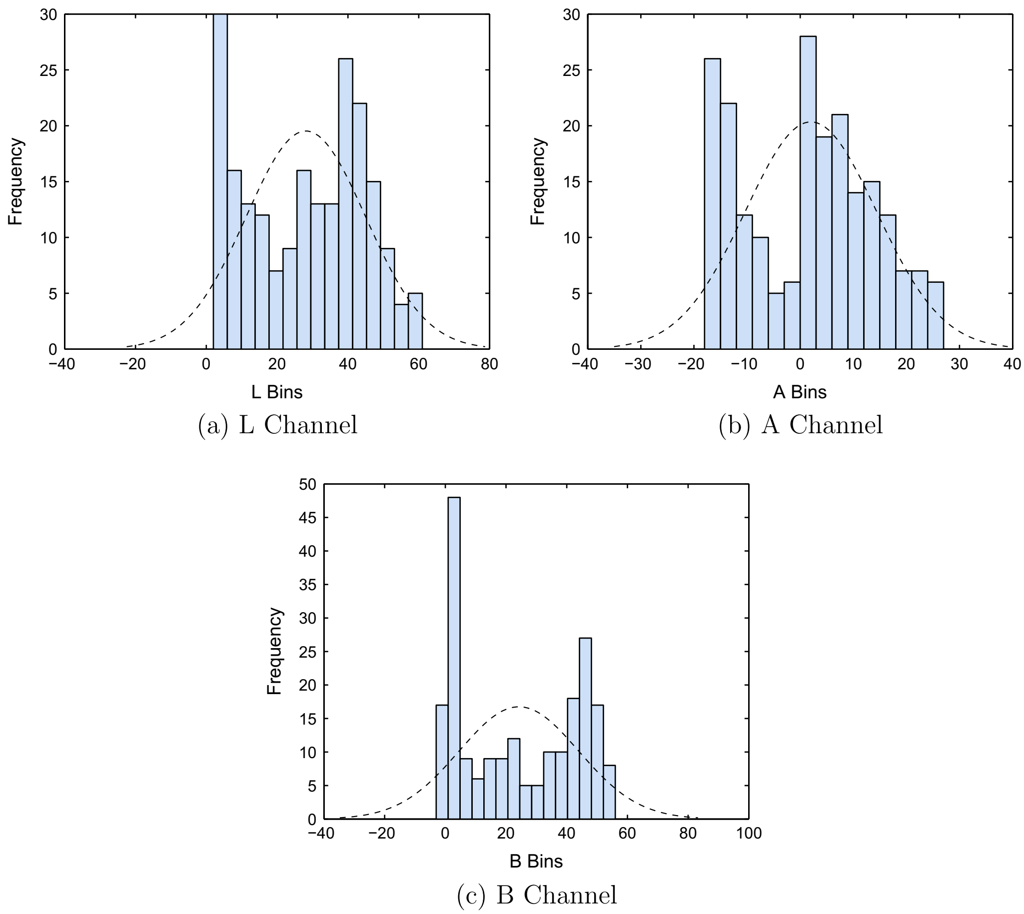

Fig. 10. Distributions of LAB channels in olives data set.

As with the case of the separation of the two classes, it is necessary to include Lagrange multipliers, which leads to the following dual expression:

$$\underset{\alpha,\alpha^*\in\mathbf{R}^m}{\text{maximize}}\ W(\boldsymbol{\alpha},\alpha^*) = -\epsilon\sum_{i=1}^{m}(\alpha_i^* + \alpha_i) + \sum_{i=1}^{m}(\alpha_i^* + \alpha_i)y_i - \frac{1}{2}\sum_{i=1}^{m}\sum_{j=1}^{m}(\alpha_i^* - \alpha_i)(\alpha_j^* - \alpha_j)k(x_i, x, j)$$

$$\text{subject to } 0 \leqslant \alpha_i, \alpha_i^* \leqslant C \text{ for all } i = 1, \ldots, m, \text{ and } \sum_{i=1}^{m}(\alpha_i^* - \alpha_i) = 0$$

finally the estimation is defined as follow:

$$f(x) = \sum_{i=1}^{m}(\alpha_i^* - \alpha_i)k(x_i, x) + b \tag{4}$$

where $k(x, x*)$ is the kernel function, α_i^* and α_i support vectors and finally b is estimated using the inequation $f(\mathbf{x}_i) - y_i \leqslant \epsilon + \xi_i$. For a detailed explanation of the estimation of b see Scholkopf and Smola (2001).

Since the representative color of a fruit corresponds to a vector in $\mathbf{R}^3$ at any color model (in this case the chosen color model is the model *LAB*), a fruit samples at different stages of maturity generates a set of points in $\mathbf{R}^3$. Fig. 7(a) corresponds to samples obtained from the dataset of the olive, while Fig. 7(b) corresponds to the data set of images of grape seed.

In this work, the creation of a color scale to a fruit corresponds to the generation model in order to estimate the central tendency of the data set. For the above task a model based on *SVR* is adopted. It provides a set of data of the form $\mathbf{x} = (x_1, x_2, x_3)$ which correspond to the *L*, *A*, and *B* channels of the representative color of a sample. To solve the proposed problem is proposed generate two models, which based on a color channel allows estimate the other 2 color channels. The first model estimates the channel *L* according to the channel *B*. The second model estimates the channel *A* according to the channel *B*. The proposed estimation models are defined by the following expressions:

$$L_E(B) = \sum_{i=1}^{m}(\alpha_i^* - \alpha_i)k(B_i, B) + b \tag{5}$$

and

$$A_E(B) = \sum_{i=1}^{m}(\alpha_i^* - \alpha_i)k(B_i, B) + b \tag{6}$$

where *B* is the value of channel *B* and corresponds to the input data of both models. L_E and A_E are the estimates for channels *L* and *A* respectively values.

For the construction of the models of estimation based on SVR the K-fold Cross Validation method is used (Sylvain and Alain, 2010) which is widely used in the literature. This method of model selection consists on dividing the sample set in *K* disjoint sets. Data $K - 1$ sets for training and the remaining set are used to test. This implies that *K* training are been done. The model that has the lowest mean squared error estimation in the test set is chosen. The expression of the function of the error performance is:

$$MSE = \frac{1}{n}\sum_{i=1}^{n}(\hat{y}_i - y_i)^2 \tag{7}$$

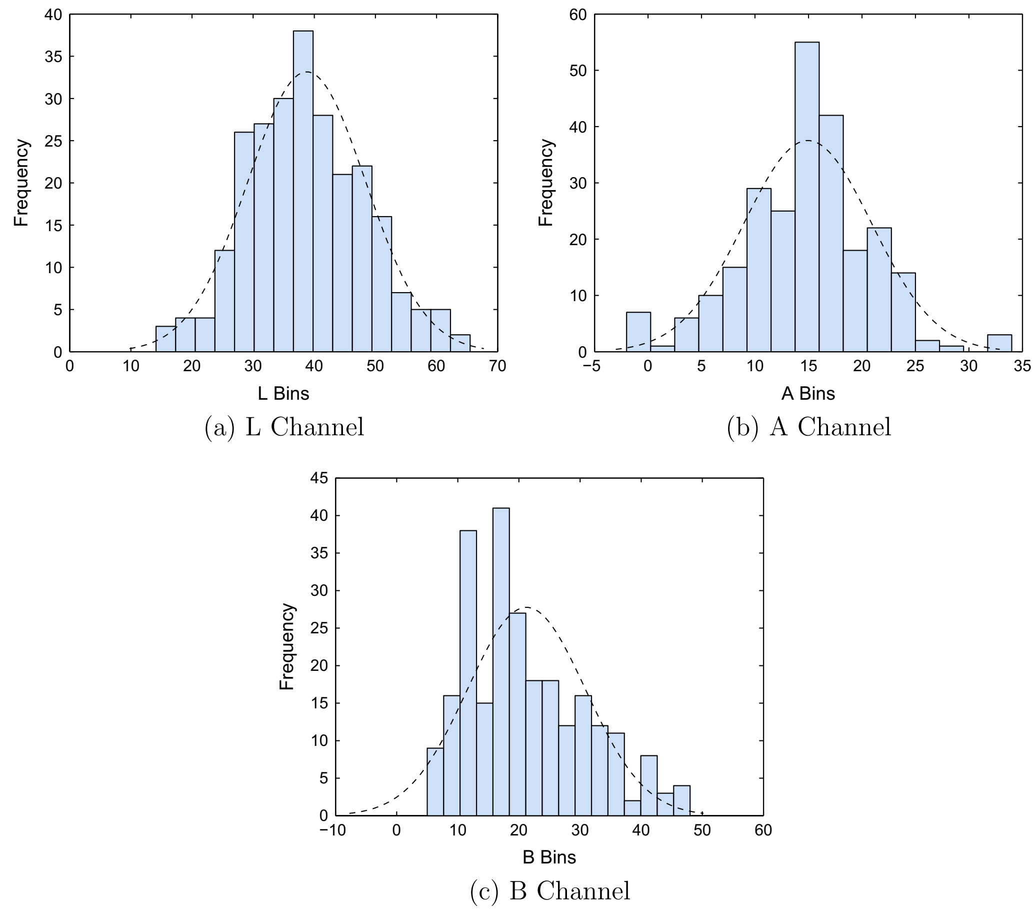

Fig. 11. Distributions of LAB channels in seeds grape data set.

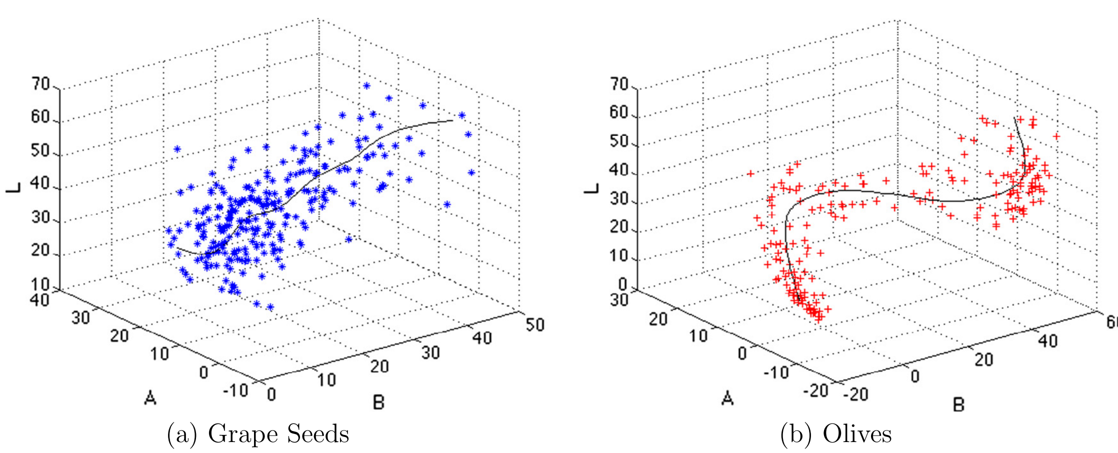

Fig. 12. Regression obtained on the two data sets.

Particularly it was considered $K = 10$, ie 10 disjoint sets (9 to training and 1 for test). It is noteworthy that the models to estimate L and A are completely independent from each other. Since there are 10 trainings for each model, the final scale is generated with the models have lower error in the test set.

The Table 1 shows the selection of the estimation models to the data from olives. The first column corresponds to the set of selected test, the second column the error estimation for L and the third column the error estimation for A. The model considered for the generation of the scale is the combination of the models with minor error estimation, which are highlighted in bold. Table 2 is the equivalent of the above table but seed data.

It is worth mentioning that the color scales were generated methodologically, which ensures appropriate estimation models.

3. Results and discussion

Given the existing relationship between color and the degree of maturity in the fruit, two data sets were considered, the first

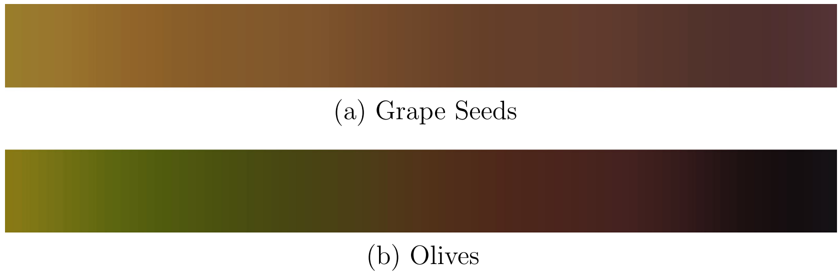

Fig. 13. Color scales obtained with the regression model. (For interpretation of the references to colour in this figure legend, the reader is referred to the web version of this article.)

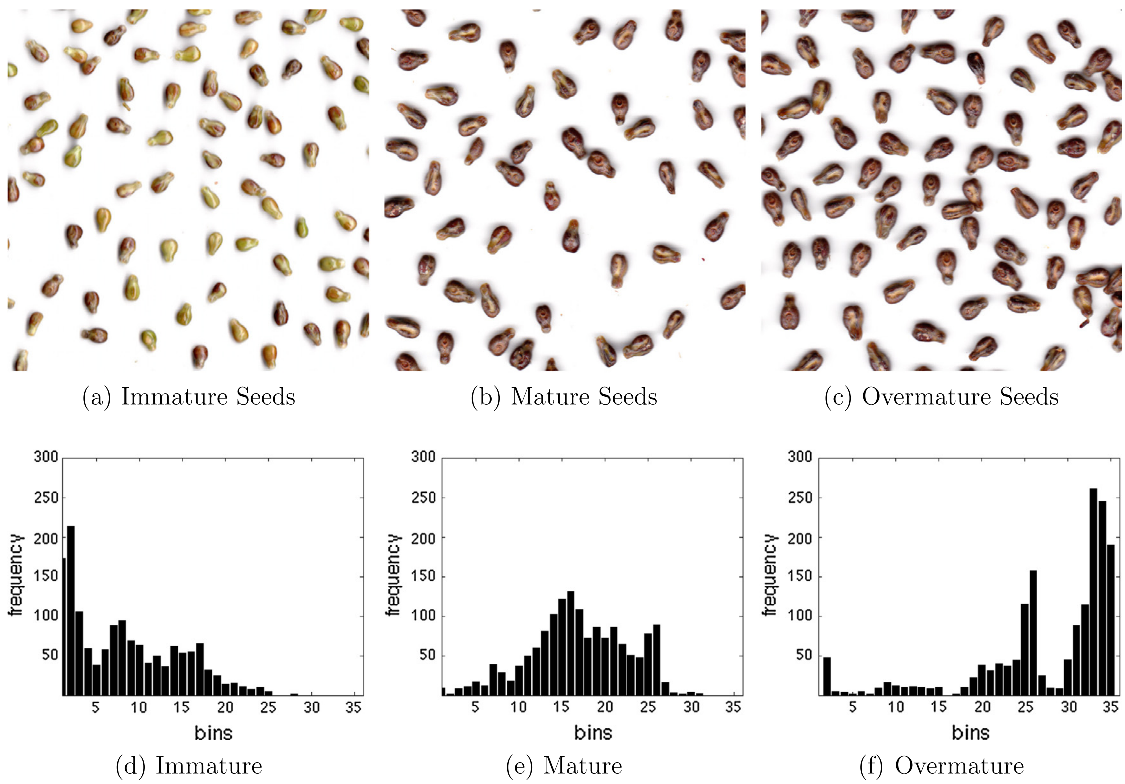

Fig. 14. Association between the color scale and maturity. (a)–(c) correspond to immature, mature and overture seeds. (d)–(f) the respective histograms associated with each maturity grade. These histograms were generated by dividing the color scale in 35 bins. (For interpretation of the references to colour in this figure legend, the reader is referred to the web version of this article.)

corresponds to the olive fruit samples during different dates in its harvest period. Fig. 8 shows some examples of colors that is taking the olive during maturation period.

In addition to the previous set of data, images corresponding to the grape seeds were used. This dataset was chosen due to have been recently proposed several methods to estimate the degree of phenolic maturity in the grapes based on images of the seed given the existing relationship between the appearance of this and the fruit maturity. Fig. 9 shows the appearance that is taking the seed during its different phenolic stages.

3.1. Sample characteristics

In this section the characteristics of each samples are presented. The olives data set contains 250 samples, where each sample is a *LAB* image. Fig. 10 shows the distribution of the sample for each color channel in *LAB* model. Fig. 10(a) shows the distribution of the *L* channel, where the mean $\mu = 28.123$ and standard deviation $\sigma = 16.872$. Fig. 10(b) shows the distribution of the *A* channel, where the mean $\mu = 2.023$ and standard deviation $\sigma = 12.351$, and finally Fig. 10(c) shows the distribution of the *B* channel, where the mean $\mu = 24.238$ and standard deviation $\sigma = 19.668$.

The seeds grape data set contains 200 samples, where each sample is a *LAB* image. Fig. 11 shows the distribution of the sample for each color channel in *LAB* model. Fig. 11(a) shows the distribution of the *L* channel, where the mean $\mu = 38.765$ and standard deviation $\sigma = 9.657$. Fig. 11(b) shows the distribution of the *A* channel, where the mean $\mu = 14.936$ and standard deviation $\sigma = 5.980$, and finally Fig. 11(c) shows the distribution of the *B* channel, where the mean $\mu = 21.228$ and standard deviation $\sigma = 9.650$.

3.2. Color scales analysis

The color scales that are presented in this section were made using data sets presented in the previous section and the model presented in Eqs. (5) and (6). Fig. 12 shows the results of the regression applied to the two datasets. In both cases it can be seen how the generated curve interpolates correctly all points.

Having obtained the curves was moved to the construction of the color scale. It contains 100 possible colors that can have the fruit during the maturation process. This scale can be observed in Fig. 13. Fig. 13(a) corresponds to the scale obtained from grape seeds and Fig. 13(b) to the corresponding to olives.

These results allow us to develop an automatic method of generating color scales for fruits, which can be used to establish stages of maturity for any fruit, not necessarily two classifications are used as usual.

Given the scales presented in Fig. 10, it is possible to associate these to different stages of maturity present in the fruits. To demonstrate that scales associate the color maturity properly, the scale was divided into 35 bins, in order to perform a histogram of colors that characterize various phenolic states. Then the segmented pixels of each image are associated with bin to compute the lower Euclidean distance.

Fig. 14 shows the association of the color scale to the state maturity of the grapes. Three stages of maturity were defined by a human expert: Mature, Immature and overmature. Fig. 14(a)–(c) shows seed images obtained at different periods of harvest. Fig. 14(a) corresponds to immature seeds, Fig. 14(b) to mature seeds and finally Fig. 14(c) to seeds overmature. Can be seen how the color changes significantly as the fruit matures.

The relation of the color scale with maturity are observed clearly in the histograms presented in Fig. 14(d)–(f). In these histograms can be seen a further clustering of data to the left in the case of immature seeds, and as the phenolic maturity progresses, bins on the left are those with greater amount of pixels associated.

As was seen in Fig. 14, the color scale generated allows to perform a correct representation of the maturity of fruits in which the color is influential factor in determining the optimal harvest point.

4. Conclusions

In this paper was proposed a development of a method for automatic determination of color scale for fruits using support machines. The method was conducted in the first instance obtaining a large number of samples, over which was applied segmentation. Later in each image the representative color in the *LAB* model was obtained. Step back two regression models were generated for predicting based on a channel the other two. Finally, a continuous curve was produced, which allows to generate continuous scales color.

Based on the results it can be seen that the generated scales can be used to establish various phenolic states on the fruit, not just two classes (mature and immature) as traditionally done.

This work has presented a computational methodology to create fruit color scales. It is noteworthy that the representativeness of the created scales can be improved considering samples from several harvest seasons.

Finally it is worth mentioning that build this type of scale provides a tool to define different phenolic pre-harvest stages, which may be of interest to the human expert, given the relation between phenolic stage and existing chemical substances in the fruit. Additionally, it is noteworthy that this method is simple and inexpensive to implement compared to other tools such as colorimeters or other associated equipment for this process.

Acknowledgments

This work is funded entirely by FONDEF IDeA CA12i10236: Estimación de la Madurez Fenólica de la Uva basada en Imágenes de la Semilla (Grape Phenolic Maturity Estimation based on Seed Images). Marco Mora, Claudio Fredes, Sergio Hernandez. National Commission for Scientific and Technological Research (CONICYT), Chilean Government.

References

Avila, F., Mora, M., Fredes, C., 2014. A method to estimate grape phenolic maturity based on seed images. Comp. Electron. Agricult. 101, 76–83.
Brosnan, T., Sun, D., 2002. Inspection and grading of agricultural and food products by computer vision system – a review. Comp. Electron. Agricult. 36, 193–213.
Changyong, L., Qixin, C., Feng, G., 2009. A method for color classification of fruits based on machine vision. WTOS 8, 312–321.
Choi, K., Lee, G., Han, H., Bunn, J., 1995. Tomato maturity evaluation using color image analysis. Trans. ASAE 38 (1), 171–176.
Cortes, C., Vapnik, V., 1995. Support-vector networks. Mach. Learn. 20, 273–297.
Dah-Jye, L., Archibald, J.K., Chang, Y., Greco, C.R., 2008. Robust color space conversion and color distribution analysis techniques for date maturity evaluation. J. Food Eng. 88, 364–372.
Diaz, R., Faus, G., Blasco, M., Blasco, J., Molto, E., 2000. The application of a fast algorithm for the classification of olives by machine vision. Food Res. Int. 33 (3), 305–309.
Fredes, C., Bennewitz, E.V., Holzapfel, E., Saavedra, F., 2010. Relation between seed appearance and phenolic maturity, a case study using grapes cv. carmenere. Chil. J. Agricult. Res. 7 (3), 1092–1098.
Garitta, L., Hough, G., Hulshof, E., 2008. Determining optimum ripening time of fruits by applying survival analysis statistics to consumer data. Food Qual. Pref. 19, 747–752.
Gevers, T., 1999. Color-based Object recognition. Patt. Recog. 32 (3), 453–464.
Guzmán, E., Baeten, V., Pierna, J.F., García-Mesa, J., 2013. Infrared machine vision system for the automatic detection of olive fruit quality. Talanta 116, 894–898.
Hanbury, A., Serra, J., 2011. Mathematical morphology in the CIELAB space. Image Anal. Stereol. 21.
Intaravanne, Y., Sumriddetchkajorn, S., Nukeaw, J., 2012. Cell phone-based two-dimensional spectral analysis for banana ripeness estimation. Sensors Actuat. B: Chem. 168, 390–394.
Lee, S.M., Lee, K.T., Lee, S.H., Song, J.K., 2013. Origin of human colour preference for food. J. Food Eng. 119, 508–515.
Mazur, S.P., Nes, A., Wold, A., Remberg, S.F., Martinsen, B.K., Aaby, K., 2013. Effects of ripeness and cultivar on chemical composition of strawberry (fragaria × ananassa duch.) fruits and their suitability for jam production as a stable product at different storage temperatures. Food Chem.
Mendoza, F., Aguilera, J., 2004. Application of image analysis for classification of ripening bananas. J. Food Sci. 69.
Otsu, N., 1979. A threshold selection method from gray-level histograms. IEEE Trans. Syst., Man Cybernet. 9, 62–66.
Pace, B., Cefola, M., Renna, F., Renna, M., Serio, F., Attolico, G., 2013. Multiple regression models and computer vision systems to predict antioxidant activity and total phenols in pigmented carrots. J. Food Eng. 117 (1), 74–81.
Palafox-Carlos, H., Yahia, E., Islas-Osuna, M., Gutierrez-Martinez, P., Robles-SÃ!nchez, M., GonzÃ!lez-Aguilar, G., 2012. Effect of ripeness stage of mango fruit (mangifera indica l., cv. ataulfo) on physiological parameters and antioxidant activity. Sci. Horticult. 135, 7–13.
Pedreschi, F., Leon, J., Mery, D., Moyano, P., 2006. Development of a computer vision system to measure the color of potato chips. Food Res. Int. 39 (10), 1092–1098.
Ristic, R., Iland, P.G., 2005. Relationships between seed and berry development of vitis vinifera l. cv shiraz: developmental changes in seed morphology and phenolic composition. Aust. J. Grape Wine Res. 11, 43–58.
Salvador, E., Cavallaro, A., Ebrahimi, T., 2001. Shadow identification and classification using invariant color models. In: Proceedings of IEEE International Conference on the Acoustics, Speech, and Signal Processing, vol. 03, pp. 1545–1548.
Sant'Anna, V., Gurak, P.D., Marczak, L.D., Tessaro, I.C., 2013. Tracking bioactive compounds with colour changes in foods – a review. Dyes Pig. 98, 601–608.
Scholkopf, B., Smola, A.J., 2001. Learning with Kernels: Support Vector Machines, Regularization, Optimization, and Beyond. MIT Press, Cambridge, MA, USA.
Slaughter, D., Crisosto, C., Tiwari, G., 2013. Nondestructive determination of flesh color in clingstone peaches. J. Food Eng. 116, 920–925.
Sylvain, A., Alain, C., et al., 2010. A survey of cross-validation procedures for model selection. Stat. Surv. 4, 40–79.
Vanloot, P., Bertrand, D., Pinatel, C., Artaud, J., Dupuy, N., 2014. Artificial vision and chemometrics analyses of olive stones for varietal identification of five French cultivars. Comp. Electron. Agricult. 102, 98–105.
Wang, Q., Wang, H., Xie, L., Zhang, Q., 2012. Outdoor color rating of sweet cherries using computer vision. Comp. Electron. Agricult. 87, 113–120.
Wu, D., Sun, D., 2013. Colour measurements by computer vision for food quality control – a review. Trends Food Sci. Technol. 29, 5–20.
Zhenfeng, L., Ning, W., Raghavan, G.V., Vigneault, C., 2009. Ripeness and rot evaluation of tommy atkins mango fruit through volatiles detection. J. Food Eng. 91, 319–324.